

Study on Waveform and Frequency Spectrum Properties of Geological Radar for Middle Weathering Limestone Surrounding Rock

Xia Wu*

School of Architecture Engineering, Jiangxi College of Applied Technology, Ganzhou, 341000, China
*Corresponding author:2181049849@qq.com

Abstract: In order to more accurately and objectively to carry out the geological radar field detection for middle weathering limestone surrounding rock, based on Zhengfeng highway tunnel of Ganxian-Xingguo expressway in Jiangxi province, the geological radar with type of LTD-2000 was adopted to execute the field detection to get the original interpretation images. The original images were preprocessed by filtering, background removal and speed transformation to eliminate the interference signal. RADAN7.0 geological radar special analysis software was used to analyze the characteristics of the reflected signal, amplitude and frequency spectrum of the interpreted images. The results show that when the water content is greater than 36%, the strong reflection characteristics of the interpreted images are obvious, the average amplitude is greater than 0.65, the spectrum is dispersed and the main frequency is greater than 75MHz. When the water content is greater than 40%, the weak reflection characteristics of the interpreted images are obvious, and a large number of dense point-like reflection signals are visible. Besides, the maximum amplitude is less than 0.5 and the main frequency is less than 45MHz under this condition, so the low frequency characteristics are obvious. The study can provide certain reference for geological radar advanced detection in limestone surrounding rock.

Keywords: Tunnel, Limestone, Geological radar, Waveform properties, Water content

1. Introduction

When constructing tunnels in limestone areas, unfavorable geological bodies such as fracture zones, faults and karst caves are easily encountered [1]. In order to reduce construction risk and ensure construction safety, advanced detection technology represented by geological radar has been widely used in tunnel construction stage and is an important means to identify various unfavorable geological bodies. In order to improve the accuracy of geological radar detection, domestic and foreign technicians and scholars have carried out relevant research in theoretical exploration and engineering application, and have achieved rich results. Shiru Wen based on a highway tunnel under construction, on the theory of electromagnetic wave footprint limit, by optimizing the detection parameters and adjusting the layout of the detection grid, improved the detection method of the side wall cave in front of the tunnel working face, and established a reliable field detection scheme [2]. Based on the Yaozhai tunnel of Liuzhai-Hechi expressway and the trigonometric function conversion model, Xia Wu proposed a geological radar detection technology for fault fracture zone. The actual construction shows that it has high accuracy [3]. Liming Zhou simulated the attribute characteristics of geological radar images of three typical bad geological bodies, and obtained the interpretation standard of the measured images. Based on the geological sketch of three tunnels, the water-bearing caves, cavity caves and corrosion fracture zones were successfully detected [4]. Undoubtedly, the above research has important theoretical and practical value for improving the detection reliability of geological radar.

However, most of the above studies did not classify the surrounding rock according to the water content and weathering degree, while the water content and weathering degree of surrounding rock are exactly the important factors affecting the electromagnetic wave propagation characteristics of geological radar. Obviously, it is easily to limit the practical promotion and application of the above research. Therefore, based on the Zhengfeng tunnel of Ganxian-Xingguo expressway in Jiangxi province, the waveform and frequency spectrum characteristics of geological radar for middle weathered limestone with different water contents are analyzed on the basis of theoretical analysis and field detection, so as to provide relevant reference for the field detection and interpretation analysis of

geological radar during the construction period of limestone tunnel.

2. Detection Principle of Geological Radar

Geological radar belongs to electromagnetic pulse exploration technology, which has the characteristics of high precision, convenient operation and strong timeliness. In recent years, it has been widely recognized and applied in related fields of civil engineering. The complete geological radar system includes three parts, namely, control computer, signal transmission cable and electromagnetic wave transmitting antenna. In the field measurement, the electromagnetic wave transmitting antenna will emit the incident electromagnetic wave with initial main frequency, energy and phase to the target soil (rock) layer according to the setting instructions and parameters in the control computer.

The rock and soil mass in natural state is not homogeneous isotropic, and its conductivity and magnetic permeability have significant spatio-temporal variability. According to the basic propagation characteristics of electromagnetic wave, electromagnetic wave will produce reflection and refraction at the interface of conductivity and magnetic permeability, and the difference of conductivity will directly affect the main frequency, phase and amplitude of reflection wave [5]. Accordingly, the physical properties of the target soil layer can be predicted by analyzing the physical characteristics of the reflected wave.

In recent years, the relevant theories and application studies in China and abroad have proved that compared with the prediction techniques such as transient electromagnetic method and seismic wave reflection method, the geological radar has good sensitivity and high resolution to the cavities, broken zones, water and other targets in the soil and rock layer, and has become the preferred technology for short-range advanced detection. The basic detection principle of geological radar is shown in Figure 1.

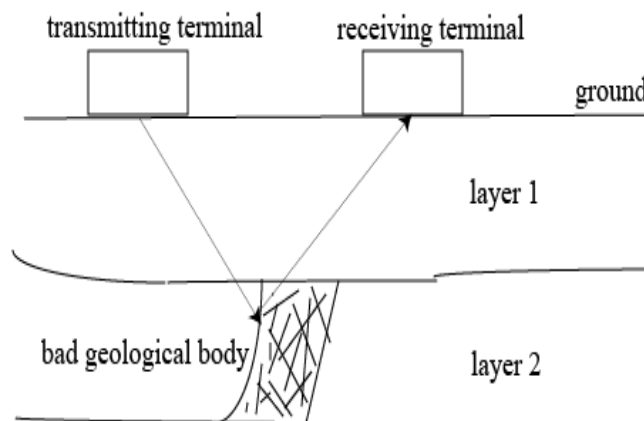


Figure 1: Sketch of detection principle of geological radar

3. Project Overview and Field Detection

3.1. Project Overview

Ganxian-Xingguo expressway is an important transportation hub connecting Xingguo county and the main city. According to the report provided by the geological survey department, the highway belongs to the southern subtropical monsoon climate area, and the rainfall is rich. The annual average precipitation is 1230.0 mm. The stratum structure along the highway is relatively simple, and the bedrock is exposed in most sections. Typical structures such as water and soil cave are visible. The surface shallow deposits are mainly silty clay, clay and gravel in the quaternary residual slope, and the bedrock is limestone. The peak ground motion acceleration in this region is less than 0.05 g, and the corresponding basic seismic intensity is less than VI. There was no obvious uplift or collapse in the terrain, no large geological structure traces were found, and no geological structures such as faults and folds were revealed by drilling, indicating that the structure was stable. The vegetation of mountains is developed, mostly trees, shrubs and bushes, and vine ferns are also visible.

The groundwater is mainly quaternary loose layer pore water and bedrock fissure water, and it is

non-corrosive to concrete and has good quality.

3.2. Field Detection

LTD-2000 geological radar was used for field detection to obtain the original detection images of limestone rock with middle weathering under different water contents. In order to facilitate subsequent analysis and statistics, the original files were numbered according to the detection date and orders, and the weathering degree of surrounding rock and the excavation mileage of working face were recorded in detail. In order to accurately obtain the water content of surrounding rock, the core was obtained by drilling method at the end of field detection. The depth and diameter of drilling was 60cm and 40mm respectively. Since the evaporation will lead to the loss of water in the core and affect the measurement results, all cores were sealed with plastic film and sent to the resident geotechnical laboratory for water content measurement in time. The number of boreholes on each working face was 8. Finally, the arithmetic average of all core water content was taken as the final water content of the surrounding rock [6-8].

Table 1 shows some field detection parameters of geological radar and the parameters not listed in the table are all the default values recommended by the system.

Table 1: Detection parameters

No.	Parameters	Values
1	Center frequency of antenna (MHz)	100
2	Emissivity (KHz)	100
3	Superposition coefficient	5
4	Time window (ns)	610
5	Number of gain	5
6	Filtering range (MHz)	LF HF 350 40

After the detection, the measured images were analyzed by RADAN7.0 geological radar analysis software. Due to the electromagnetic wave emitted by the geological radar is easily affected by the external electromagnetic field and metal objects, the mobile phones carried by the operation workers were closed and the interference objects such as anchor bolts, trolleys, drilling rigs and steel mesh near the working face were removed [9], [10].

4. Waveform and Frequency Spectrum Properties

4.1. When $\omega < 36\%$

When the water content (ω) is less than 36%, the strong reflection characteristics of the interpreted image are very obvious, the average amplitude is greater than 0.65, the spectrum is dispersed, and the main frequency (f) is greater than 75 MHz. Figure 2 shows the typical line-scan detection images. It can be seen that the reflected signal in the image is very clear. Even after 20m in front of the working face, the reflected signal still does not show obvious attenuation.

Studies have shown that water will enhance the conductivity and relative dielectric constant of rock and soil, thereby enhancing the attenuation rate of incident electromagnetic wave energy, and it will continue to decay with the increase of detection depth until effective reflection signals cannot be generated. In this process, the reflected signal in the detection image will gradually become blurred and spotted from a certain depth until no signal.

In addition, the reflected signal in Figure 2 is always in a continuous state, and there is no obvious signal interruption region in both horizontal and vertical directions. Before 15m, the reflected signal is very continuous and uniform, and there is no obvious fracture and dislocation in the phase axis, indicating that the incident electromagnetic wave generates good reflection in this range and the travel energy does not produce significant attenuation. When the depth exceeds 15m, the electromagnetic wave energy begins to decay, but does not affect the effective reflection signal. Obviously, there is no water-rich phenomenon in the target surrounding rock, and the rock mass is dry as a whole.

In the actual detection work, the waveform characteristics shown in Figure 2 often indicate that the target surrounding rock is broken but the water content is low. Attention should be paid to this in the future work.

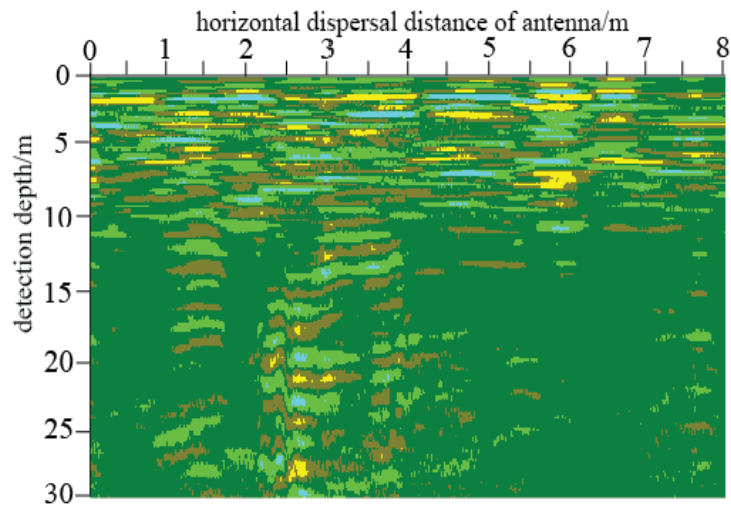


Figure 2: Line-scan image ($\omega < 36\%$)

Figure 3 shows the point-scan image corresponding to Figure 2. It can be seen that there is a strong oscillation in the single-channel reflection wave, and the reflection period does not have a specific law, and the amplitude is large, indicating that it is a strong reflection feature.

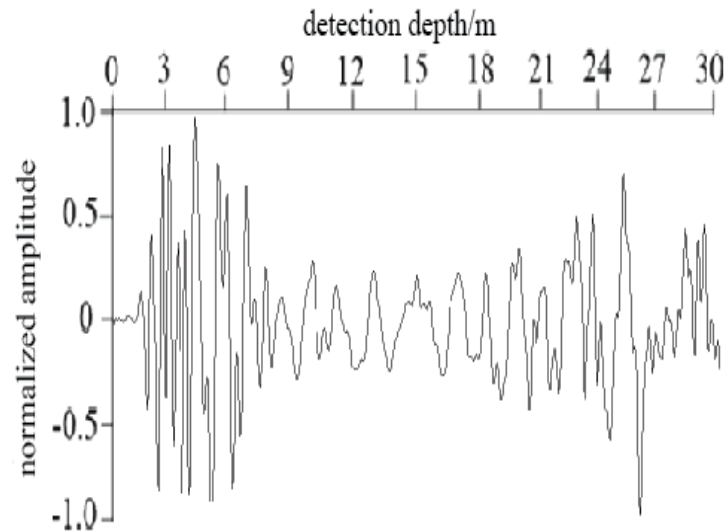


Figure 3: Point-scan image ($\omega < 36\%$)

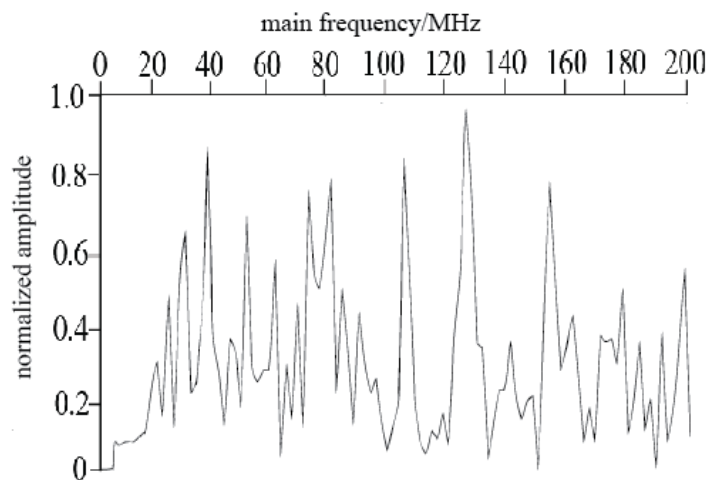


Figure 4: Frequency spectrum of wave ($\omega < 36\%$)

Figure 4 mentioned above shows the frequency spectrum of wave. It can be seen that the fluctuation

of echo main frequency is very intense and the distribution range is wide. The subsequent excavation verification showed that the internal weathering of the working face was serious, the surrounding rock was broken, the joints and cracks were developed, but it was wholly dry.

4.2. When $\omega > 40\%$

When the water content (ω) is greater than 40%, the weak reflection characteristics are very obvious, and a large number of dense point-like reflection signals can be seen. The maximum amplitude is less than 0.5, the spectrum is prominent, and the main frequency (f) is less than 45MHz indicating that the low-frequency characteristics are obvious.

Figure 5 shows the line-scan image, it can be seen that the reflection signal is very weak, almost no effective reflection signal, can only see dense “fuzzy spots”.

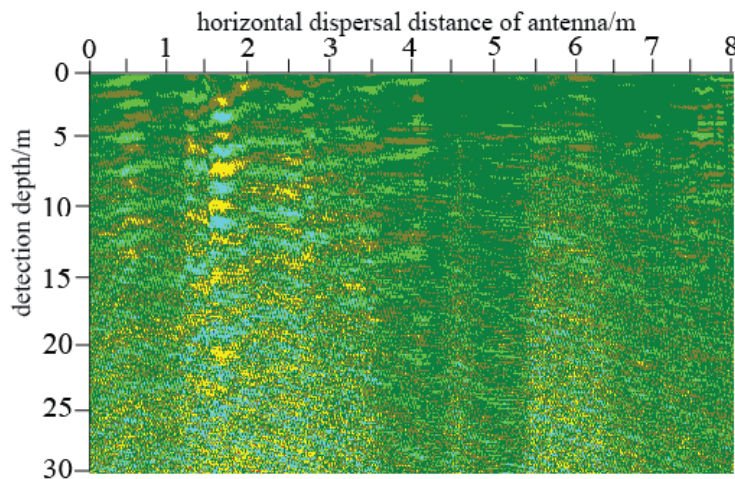


Figure 5: Line-scan image ($\omega > 40\%$)

Figure 6 shows the point-scan image. It can be seen that the single-channel reflection wave also has violent oscillation, and the reflection period does not have a specific law, but the amplitude is small, indicating that it is a weak reflection feature.

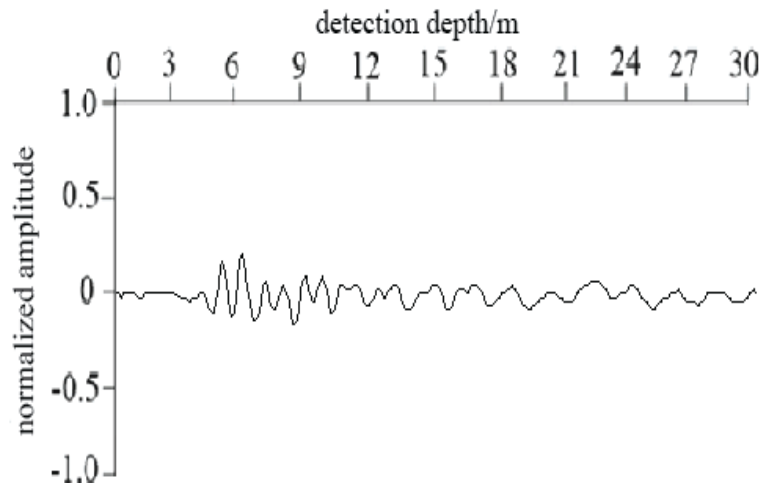


Figure 6: Point-scan image ($\omega > 40\%$)

Figure 7 shows the frequency spectrum of echo wave. It can be seen that the fluctuation of main frequency is relatively intense but the distribution range is narrow, and the value is low. The subsequent excavation verification showed that the internal weathering of the face was serious, the surrounding rock was broken and wet, diffuse water droplets can be seen with the naked eye, and most joints and cracks were filled with calcite. For surrounding rock with high water content, the frequency spectrum usually has the characteristics shown in Figure 7. Therefore, this kind of key characteristics can be used to predict the internal water content in practical work.

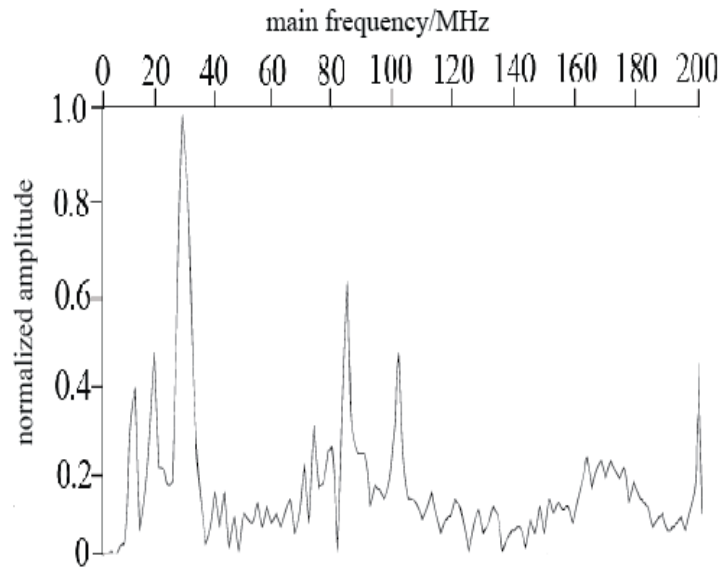


Figure 7: Frequency spectrum of wave ($\omega > 40\%$)

5. Conclusions

Based on the Zhengfeng tunnel in Ganxian-Xingguo expressway in Jiangxi province, the waveform and frequency spectrum properties of geological radar for middle weathered limestone surrounding rock with different water contents were analyzed on the basis of theoretical analysis and field detection. The conclusions are as follows:

- 1) Water content has a direct impact on the clarity of interpretation image, the amplitude and main frequency of the reflected wave. The impact of water content cannot be ignored in the post-interpretation process.
- 2) When $\omega < 36\%$, the strong reflection characteristics are obvious, the reflection signal is clear, the average amplitude is greater than 0.65, the spectrum is dispersed and f is greater than 75MHz.
- 3) When $\omega > 40\%$, the weak reflection characteristics of the interpreted image are obvious, a large number of dense point-like signals are visible, the maximum amplitude is less than 0.5, and the spectrum is prominent and $f < 45\text{MHz}$.

Acknowledgements

This work was supported in part by the Science and Technology Research Project of the Education Department of Jiangxi Province under Grant GJJ204903.

References

- [1] Xiaoyu Zi, Yusheng Shen, Shuangyan Zhu, Ningning Luo, and Jiaqi Yang. Study on the deformation failure laws and support measures for tunnels in layered phyllite [J]. *Modern Tunnelling Technology*, 2021, 58(03):196-204.
- [2] Shiru Wen, Xiaohua Yang, Xia Wu, and Xingjiao Wu. Study on Detection Method of GPR for Karst Cave on Tunnel Side Wall Ahead of Excavation Face [J]. *Journal of Highway and Transportation Research and Development*, 2014, 31(10):93-96+118.
- [3] Xia Wu. Advance forecast of tunnel fault fracture zone based on geological logging and ground penetrating radar [J]. *Journal of Henan University of Engineering*, 2019, 31(02):53-56.
- [4] Liming Zhou, Daiguang Fu, Yang Zhang, and Huaming Zhou. Forward Test of GPR Detection for Typical Adverse Geological Bodies [J]. *Modern Tunnelling Technology*, 2018, 55(04):47-52+58.
- [5] Hao Wu, Xiaohua Yang, and Shiru Wen. Study on Spectrum Characteristics of GPR for Water-rich Crushed Zone in Karstic Area [J]. *Journal of Highway and Transportation Research and Development*, 2018, 35(12):90-94+103.
- [6] J.O. Backhaus. Construction time prediction of injections in tunnel construction [J].

BAUTECHNIK, 2020, 97(09):626-636.

[7] C. Yoo, S.S. Cui. *Effect of new tunnel construction on structural performance of existing tunnel lining [J]. GEOMECHANICS AND ENGINEERING*, 2020, 22(06):497-507.

[8] Zhongqiang Sun. *RULE OF DUST MOVEMENT IN TUNNEL CONSTRUCTION AND ITS PROTECTION AND TREATMENT [J]. FRESENIUS ENVIRONMENTAL BULLETIN*, 2020, 29(12):10696-10700.

[9] Shiru Wen, Xiaohua Yang, and Yuanshu Guo. *Interpretation based on frequency spectrum energy analysis of ground penetrating radar detection image [J].Advanced Engineering Sciences*, 2020, 52(6):120-130.

[10] Zhiwen Li. *Application of GPR in Advance Geological Prediction of Tunnel [J]. Engineering Equipment and Materials*, 2020, 5(16):124-126.